SciMedCentral

Journal of Materials & Applied Science

Research Article

Adsorption Mechanism of Sodium Metasilicate on Rutile and Almandine Surfaces

Richard M Kasomo[1], Eric M Kinyua[1], Hongqiang Li[2]*, Akisa D Mwangi[4], Sammy Ombiro[4], Kyangi Joseph[1], Yangge Zhu[3] and Fatuma Rajab Mwanganga[4]

[1]*School of Mines and Engineering, Mining and Mineral Processing Engineering Department, Taita Taveta University, Voi, Kenya*
[2]*School of Resource and Safety Engineering, Wuhan Institute of Technology, Wuhan, China*
[3]*State Key Laboratory of Mineral Processing Science and Technology, Beijing General Research Institute of Mining and Metallurgy, Beijing, China*
[4]*School of Mechanical, Manufacturing and Materials Engineering, Mining, Materials and Petroleum Engineering, Department, Jomo Kenyatta University of Agriculture and Technology, Nairobi, Kenya*

***Corresponding author**
Hongqiang Li, School of Resource and Safety Engineering, Wuhan Institute of Technology, Wuhan, China

Submitted: 17 November 2023
Accepted: 04 December 2023
Published: 06 December 2023
ISSN: 2333-7133

Copyright
© 2023 Kasomo RM, et al.

OPEN ACCESS

Keywords
- Sodium Metasilicate
- Rutile
- Almandine
- Adsorption Mechanism

Abstract

Sodium metasilicate was investigated as a possible depressant in the separation of rutile from almandine. The study determined the floatability of the depressant through micro flotation tests of single and artificially mixed minerals. The adsorption behavior of sodium met silicate on the rutile and almandine surfaces was determined by the zeta potential measurement and X-ray Photoelectron Spectroscopy (XPS). The flotation tests for both single and artificially mixed minerals demonstrated that Sodium metasilicate could be an efficient depressant in the separation of rutile from almandine. Zeta potential measurements and XPS analysis depicted that more of Sodium metasilicate was adsorbed on almandine surface than that of rutile. Fe ions on the surface of almandine were the main active sites for collector attachment and adsorption. The element Si in sodium metasilicate was postulated to have contributed to depression of almandine too. The adsorption mechanism of sodium metasilicate on the surface of almandine was mainly attributed to the electrostatic interaction as well as chemical bonding.

INTRODUCTION

Rutile is a very crucial raw material for the extraction of titanium as well as the production of titanium dioxide [1]**.** Rutile is also employed in the manufacturing of: Titanium sponge, Titanium dioxide pigment, cosmetics pharmaceuticals, plastics, paper and latex rubber [2-6]. Further uses of titanium dioxide may include: military aviation, navigation, machinery, aerospace, seawater desalination and chemical industry among many other uses [7,8]. There are several processes used to upgrade and dress rutile ore which include: magnetic separation, flotation, magnetic-flotation, gravity separation and electrostatic separation [9-12]. As aforementioned, these rutile dressing methods sometimes suffer from inadequacies during the concentration process. For instances, there exists very little difference between the densities of rutile and almandine gangue [13]. In regard to this, it is almost impossible to separate the two minerals by use of gravity separation concentration method [14]. Further to this, it is worth mentioning that both rutile and almandine have similar physicochemical characteristics and as such, the successful separation of the two minerals through gravity concentration process might not be attainable [13].

In search for an effective method for separation of rutile from its gangue minerals, a combination of magnetic and froth flotation technique was developed [15]. A challenge is always encountered in this separation technique in that, quite often than not, there is always a substitution of titanium in the rutile crystal lattice occurring by iron in the form of isomorphism, and thus, rutile slimes are often wrapped by almandine-surface, hence making it very difficult for flotation-magnetic separation technique to be effective [13-16]. Froth flotation, has therefore, remained the most reliable and versatile technique in concentration and dressing of the rutile ores [17].

Reagents and their suitable schemes have remained the major challenge in enrichment of ores. Currently the main focus on rutile flotation has been designing the suitable flotation reagents which register rutile of high quality grade. Many studies in the area of rutile flotation have been concentrated on the development, modification and choice of novel collectors to enhance the floatability difference between rutile and its associated gangue so as to enhance its reparability [18-22]. However, several studies have proved beyond reasonable doubts that, no any single collector that possess enough collective as well as selective capabilities, as such depressants studies is of great interest of late. The focus on depressants has been occasioned by the fact that they help the collectors to achieve that most

required selectivity as its main function is to render the gangue mineral hydrophilic and hence impairing its flotation as well as aiding selectivity of the collector as much as possible to enhance the grade of the concentrate [11,23].

Sodium metasilicate has remained as one of such depressant in mineral processing operation [24]. It is has proved to be a versatile and non-toxic, as well as a low-cost multifaceted flotation reagent available in many forms and for a wide range of industrial applications [25]. Sodium metasilicate has been commonly utilized in mineral concentrators as a dispersant, rheology modifying, as well as an inorganic depressant whose effectiveness has been reported in many studies [25]. Additionally, sodium metasilicate has found its application in selective separation of hematite from quartz by reverse flotation where promising results were revealed and recorded [26]. Similarly, it was used as a depressor while sodium operate was on the other hand employed as a collector in the flotation separation of fine fluorite from fine quartz. The results revealed that sodium metasilicate helped to depress the hetero-coagulation and therefore improved the separation efficiency in the beneficiation of mixed binary minerals [27]. It is further utilized as an effective depressant in direct flotation of apatite from siliceous phosphate ore using fatty acids and promising results were posted as well [28]. Additionally, it can be used as an activator because it helps in the reduction or elimination of the deleterious effects of slimes on flotation [29]. Furthermore, sodium metasilicate has been used in grinding unit operation as it helps in lowering the viscosity and provides finer grinding or increases throughput for the same particle sizes [30].

Several other studies have been conducted to investigate the effect of sodium metasilicate as a possible dispersant as well as a depressant with different mineral ores whose response and best results have been positively recommended [31-33]. However, despite the above mentioned studies, there is no reliable literature and information on the proper mechanism of how sodium metasilicate depresses iron-bearing silicate and its related minerals. For instance, the depressing action and mechanism of sodium metasilicate on the surface of iron-containing silicate has not been systematically explained before and no enough data on the same which has been reported so far.

In this current study, the flotation behavior of rutile and almandine employing sodium metasilicate as a depressant, octadecylamine, polyoxyethylene ether (AC1815) as the collector is investigated in details is using micro-flotation tests for single as well as the artificially mixed minerals. The adsorption phenomenon of sodium Metasilicate on the almandine and rutile surfaces was clearly unraveled by use of contact angle and zeta potential measurements as well as XPS analyses. The limitation of this study will be the fact that in rutile gangue minerals the authors concentrated with almandine only and did not conduct any comparisons studies with other gangue minerals like hornblende among others.

MATERIALS AND METHODS

Materials

The representative sample of rutile for this research work was obtained from Hainan province, China. It was a tabling concentrate, with 98 wt% TiO_2 contents. The sample preparation included grinding it in a porcelain ball mill and subsequently screened it by a wet sieve to obtain the final size fraction of -150 +58 μm suitable for micro flotation and other tests. Almandine sample on the other side was a magnetic concentrate procured from Donghai country, Jiangsu province in China which had 97 wt% purity. Its preparation entailed the dry magnetic separation and then vibration mill. Finally, the ground sample was screened to obtain a size fraction of –150 +58 μm. The bulk constituents of the samples were analyzed by chemical analysis methods, where X-ray fluorescence spectrometry (XRF) test was conducted and the results are depicted in (Table 1). Additionally, X-ray diffraction (XRD) was used to characterize the mineral compositions. The results can be found in (Figure 1a,b) respectively.

Reagents

Octadecylaminepolyoxyethylene ether (AC1815), which had 99wt% purity, was obtained from Haian Petrochemical factory in

Table 1: The chemical compositions of the rutile and almandine samples (wt. %).

Composition	Na_2O	MgO	Al_2O_3	SiO_2	CaO	TiO_2	MnO	Fe_2O_3
Rutile	-	-	-	0.42	0.02	98.03	-	0.41
Almandine	0.729	5.119	17.701	38.591	9.046	1.703	0.497	26.276

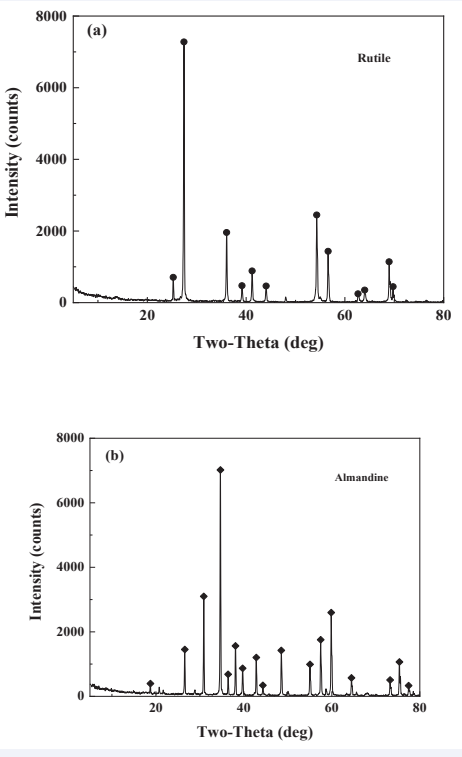

Figure 1 XRD pattern of a. Rutile; b. Almandine.

Jiangsu province, China. Moreover, dilute solution of hydrochloric acid (HCl) and sodium hydroxide (NaOH) were employed for pH adjustment and moderation. Analytical grade reagent potassium nitrate (KNO_3) was used to maintain the ionic strength in zeta potential measurement. Sodium Metasilicate was of analytical grade, purchased from Sinopharm Chemical Reagent Co., Ltd., China. Deionized water (18.25 MΩ) obtained from a Milli-Q Direct 16 (Millipore Q, USA) was used throughout the experiments.

Methods

Micro-flotation tests: The micro-flotation tests were conducted using an XFG-type flotation machine with a 40 ml cell and an impeller speed of 1700 rpm as can be seen in [Figure 2]. The Micro-flotation experiments in this study were carried out in a 40 mL-Plexiglas cell. The reagents addition orders and the time of conditioning were as follows: The pure mineral sample (3.0 g) was placed in a Plexiglas cell, which was then filled with 40 mL deionized water (Millipore deionized, resistivity of 18.25MΩ cm). The pulp was conditioned for 3 mins. The depressant was added and then conditioned for 3 mins. The collector was added to the slurry and it was further conditioned for another 3mins before the frother was added to the pulp. After the frother was added to the mixture, it was conditioned for another 3 mins and the flotation was then conducted.

For artificially mixed minerals, the mass ratio of the rutile and almandine (binary mixture) was 1:4 (0.6 g Rutile + 2.4 g Almandine). The impeller speed was fixed at 1700 r/min.The pH of the suspension was modified by the addition of HCl or NaOH as required, after that process, filtration was conducted, and then the concentrate was weighed and dried for final analysis. For single mineral flotation, the mineral recoveries were calculated based on the dry weights of the concentrates (M_1) and tails (M_2), see equation (1). The results of each micro-flotation test were measured three times, to sustain the reproducibility, congruity, and repeatability of the experimental parameters and data [34], with the average being reported as the final tally.

$$\text{Floatability(F)} = \frac{M_1}{M_1 + M_2}(\%) \qquad (1)$$

Figure 2 Schematic of XFG-type flotation machine.

Where floatability F, is the mineral flotation recovery (%), M_1 is the weight of concentrate (g), M_2 is the weight of tailings (g) [35]. For artificially mixed minerals flotation, the concentrate was assayed for TiO_2. Rutile recovery (%) was calculated based on the grade (%) of TiO_2 and the mass of the concentrate. The equation (2) was used to calculate the above percentage recovery.

$$\text{Re} = \frac{cC}{(cC + tT)} \times 100 \qquad (2)$$

Where, Re: the recovery of valuable mineral recovered from raw ores to concentrate, and c is the content of target material in the concentrate (product fraction); t: the content of target material in the tailing (reject fraction); C: mass of concentrate (product fraction); T: mass of the tailing (reject fraction) [36,37].

Contact angle measurements: Solid-liquid contact angle is basically used as a quantitative measure of wettability of a solid by a liquid [38, 39]. The contact angle measurement in this study work was conducted using a Kruss drop shape analysis system (DSA 10-MK2, Germany). The sessile drop method was particularly used to determine the contact angle of water on the pressed mineral pellet surface with a 10 mm diameter. The samples were prepared using the same procedure as in single mineral flotation. The pellets were prepared using 0.3 g of the powdered mineral under a pressure of 2876 psi (196 atm) (ICL International Crystal Laboratories, USA) for 5 minutes. A drop of distilled water would be placed onto the surface of the pressed pellet and a set of microscopic images of the drop and the pellet were taken immediately. Then one image with the momentary view was taken to determine the contact angle by fitting a tangent to the shape of the sessile drop on the microscopic image. The measurements were done in triplicate with average value being recorded as the final.

Zeta potential measurements: The effect of depressant adsorption on surface charges of rutile and almandine particles was examined using a Zetasizernano Zs90 (Nano series, Malvern Instruments, UK). These measurements were based on electrophoresis technique with the equipment being supplied by Malvern Zetasizer Nano (2000). For this, a suspension of the particles was prepared by mixing 0.01 g (< 5 μm size) of the desired mineral with 45 mL of the KNO^3 (1 × 10-3 mol/L) as the background electrolyte solution. The pH of the suspension was then modified by use of HCL/NaOH solution for 5 min conditioning time. After the pH adjustment, reagent was added and conditioned for 10 min. After completion of conditioning times, the coarse particles were then allowed to settle for about 5 min. Thereafter, the pH of suspension was noted and the solution containing ultra-fine particles was transferred to a for zeta potential capillary cell for measurements. At least three measurements were made for each experimental condition and the average calculated as the final value at that given condition.

XPS analysis: X-ray Photoelectron Spectroscopy (XPS) is a versatile surface analysis technique used for compositional and chemical states analysis, it can also be employed to provide information and other characteristics of the flotation reagents

[40,41]. XPS study has a capability of detecting the chemical composition of the surface and depth of (< 10 nm). In this study work, the XPS data was obtained using a Thermo Fisher ESCALAB 250 XPS system (American Thermo Fisher Scientific).

The samples for XPS tests for both minerals were prepared as following this procedure: 3.0 g single mineral (particle size of 5 μm) was added into sodium metasilicate solution with an appropriate and desired concentration. Then, the pulp was agitated in a mechanical flotation cell for 20 minutes to allow adequate time for effective adsorption process. The stirring speed was basically set at 1700 rpm. Then, the solid samples were washed three times using DI water at the required pH. These washed samples were then vacuum dried at 60°C for more than 12 hours prior to XPS analysis.

RESULTS AND DISCUSSION

Single Mineral Flotation

Collector concentration: [Figure 3] shows the relationship between the collector concentration and the floatabilities for single minerals, rutile, and almandine. As AC1815 concentration increased from 3.5 mg/L to 28 mg/L rutile floatabilities also increased from 68.16% to 95.48% respectively and thereafter a flatten out. The floatability for almandine on the other hand increased from 0.55% to 49.99% at optimum collector dosage. This results were in agreement with the findings [23]. The increase of these floatabilities could have been attributed to promotion floatabilities of rutile and almandine.

Effect of pulp pH: The action of sodium metasilicate in selective flotation depends mainly on the pH of the pulp/slurry [42, 43]. The results for determination of the best pH for collector is displayed in [Figure 4]. In this [Figure 4], AC1815 depicts a good collector performance for rutile floatability at a relatively wide pH range of 2-8. At pH 2 the floatability was at 23.9%, but when the pH was adjusted to 4, the floatability of rutile increased to 97.5%. The increase of pH = 6, the floatability started to decrease and later at pH 10, the floatability recorded its lowest percentage.

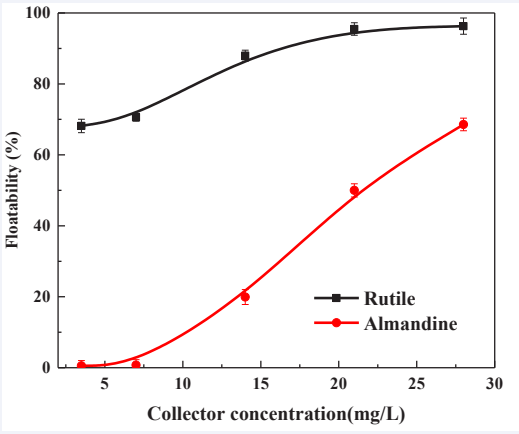

Figure 3 Effect of AC1815 concentration on floatability of rutile and almandine. (Pulp pH: 6.0).

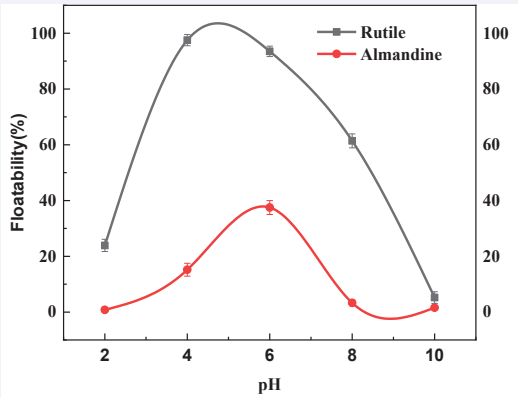

Figure 4 Effect of pulp pH on floatability of rutile and almandine. (AC1815 concentration: 21 mg/L)

Almandine similarly registered the same trend. Floatabilities were very reasonable within the pH ranges 4-6. Consequently, very low floatabilities were registered in too much acidic or too much alkaline environments and conditions of pH 2 (floatability of 0.8%) and pH 10 (floatability of 1.58%) respectively. The optimum results were registered at pH = 4 which recorded the floatability of 37.5% corresponding to good floatability for rutile as well.

We could attribute this outcome to the fact that at those extreme pH conditions, the adsorption of collector (AC1815) onto almandine might have been sharply reduced. Further to the above explanation, the reduction on the collector adsorption on almandine could have been connected to the fact that, in too much acidic condition, mineral surface is positively charged and the cationic collector was also positively charged hence electrostatic repulsion. Also at pH 10, the environment was too much alkaline, cationic collector exists in molecular form, no electrical attraction occurred between collector and minerals surface with highly negatively charged surface [44-46]. Similarly, at pH values above 6, the predominant silicic specimens in solution are basically [$SiO(OH)_3^-$] and [$SiO_2(OH)_2^{2-}$], which could have been specifically adsorbed onto the negative almandine surface forming an insoluble layer which prevented and blocked the collector's adsorption, and hence leading to decreased floatability.

Effect of sodium metasilicate concentration: [Figure 5] shows the results of sodium metasilicate influence on single minerals floatabilities. It can be clearly observed that at 0×10^{-6} mol/L, the floatability of rutile is 92.48% and increasing the depressant dosage to 3×10^{-6} mol/L, the floatability would still remain above 89%, this clearly indicated that Na_2SiO_3 did not have an adverse depressing effect on rutile floatability. Increasing sodium metasilicate further did not register an appreciable decrease in floatabilities of rutile. The floatabilities remained way above 85% at the highest concentration of the depressant (6×10^{-6} mol/L).

In the absence of sodium metasilicate, almandine floatability was 37.99%. Increasing Na_2SiO_3 to 3×10^{-6} mol/L, the floatability

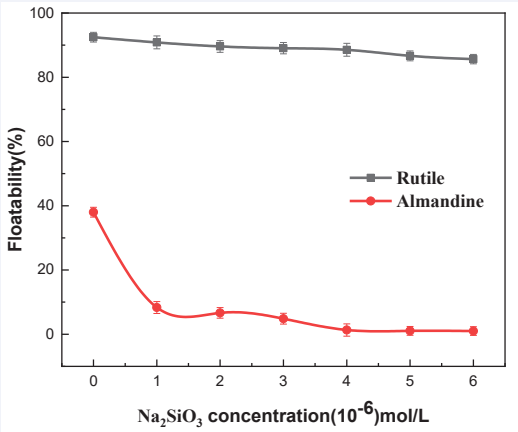

Figure 5 Effects of sodium metasilicate concentration on floatability of rutile and almandine. (AC1815:21 mg/L, pulp, pH = 6).

dropped sharply from 37.99% to 4.86% and any further increase of sodium metasilicate beyond the optimum concentration (3×10^{-6} mol/L), the floatability of almandine was negligible, this clearly shows that the material that was amenable to suppression in flotation system, had already been suppressed. So, it can be decoupled from the results, that rutile and almandine can successfully be separated by the use of AC1815 as a collector and Sodium Metasilicate (SM), as a regulator, as sodium metasilicate has a significant inhibition of almandine floatability, while its inhibition on rutile surface is very low.

Flotation of the Artificially Mixed Minerals

The influence of Sodium Metasilicate concentration on the grade and TiO_2 recovery of froth concentrate is shown in [Figure 6]. It is clearly shown that, with the increase of depressant concentration from 0 $\times10^{-5}$ mol/L, to the 2.5×10^{-5} mol/L, the recovery initially decreased from 97.79% to 92.72%, and then any further increase of the depressant dosage beyond this optimum dosage didn't have any noticeable change on the recovery indicating that 2.5×10^{-5} mol/L was considered as the optimum depressant concentration.

The grade of this flotation process on the other hand increased as the depressant concentration increased, that is, from 28.97% to 55.10% respectively. Dosage concentration of 2.5 $\times10^{-5}$ mol/L, was therefore considered to be the optimum dosage of sodium metasilicate in mixed minerals flotation, with optimum recovery at 92.72% and the corresponding grade of 55.10%. Further to that, even at high sodium metasilicate concentration, 5.5×10^{-5} mol/L the recovery remained at reasonably high percentage, that is, 85.50% which was very promising as well. Similarly, the corresponding grade was even very positive at 75.80%. This clearly demonstrated that this depressant was very effective in the flotation separation of rutile from almandine.

Results for Contact Angle Measurements

In order to reveal the difference in hydrophobicity between the almandine and rutile, contact angles measurements were conducted. (Figure 7) shows the measurements of the surface contact angle of rutile and almandine at pH = 6. The contact angles measurements of rutile without flotation chemicals treatment was measured and recorded at 37.5°, a value that concurred with the findings reported in other studies [47-49]. while that of almandine was 36.55°. This indicates that the two minerals are hydrophilic in nature. These results tend to agree with single mineral flotation which exhibited a similar floatability trend for the two minerals when collector was used.

The contact angles of rutile increased to above 70.00° from 37.50°, when treated with depressant and the AC1815 at the concentration of 21 mg/L which changed it from hydrophilic to hydrophobic form. Variations of depressant concentrations did not yield much reduction in the contact angles of rutile. The contact angle of almandine sample after being treated with

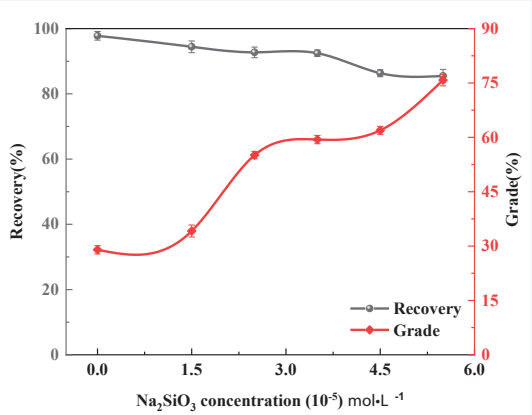

Figure 6 Recovery and grade of artificially mixed minerals as function of sodium metasilicate dosage. (with fixed total collector (AC1815) dosage of 40 mg/L, pH = 6)).

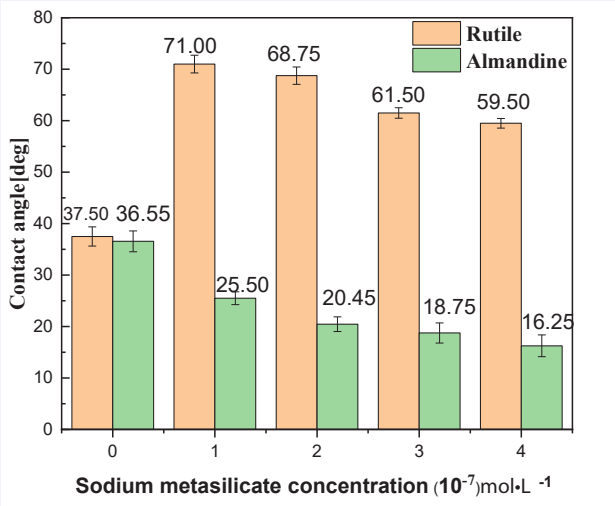

Figure 7 Contact angles on mineral surfaces as a function of sodium metasilicate concentration under different conditions: (a) Collector (ACI815) dosage =21 mg/L and (b) pH = 6.0.

collector at the same concentration as that of rutile decreased sharply at various depressant concentrations, proving that the surface of almandine was becoming more hydrophilic than that of rutile when the minerals reacted with sodium metasilicate. The above results therefore suggest that, the hydrophobic difference between the rutile and almandine surfaces was clearly enhanced when both surfaces interacted with the depressant, and consequently their further separation became much easier.

Effects of Sodium Metasilicate on Zeta Potentials of Rutile and Almandine

Zeta potential (ζ) is a measure for quantifying the magnitude of the electrical charge at the double layer, additionally it can be used to measure the charges carried by particles that are suspended in an electrolyte solution [50]. Zeta potentials results for rutile and almandine as a function of pH values were determined and are clearly illustrated in (Figure 8a,b) respectively. It can be seen from (Figure 8a) that, the Isoelectric Point (IEP) of rutile before reacting with sodium metasilicate was found to be at pH 2.5. The outcome of these finding were in concurrence with the findings [11-49]. After being treated with sodium metasilicate, the IEP did not occur within the studied pH range. The result for rutile interaction with sodium metasilicate does not display any appreciable change and it can therefore be concluded that the depressant had little effect on the surface of rutile. These results do collaborate closely with the micro flotation test.

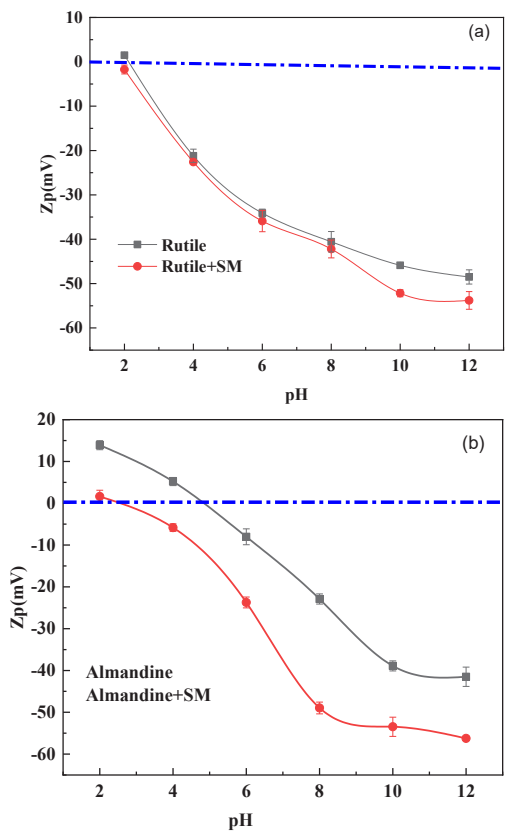

Figure 8 Relationship between Zeta potential and pH value for a. Rutile; b. Almandine.

On the other hand, the Isoelectric Point (IEP) of almandine mineral as clearly shown in (Figure 8b) was established to be 5.5. These results closely agreed with the findings [51]. After treatment with sodium metasilicate, the IEP of almandine became more negative and the IEP pH changed to 3.0. The addition of sodium metasilicate could decrease the Zeta potential values for almandine over the entire pH range tested. The probable explanation to this is the fact that sodium metasilicate negative ions, [SiO $(OH)_3^-$] and [SiO_2 $(OH)_2^{2-}$] could have been absorbed on the surface of almandine and thus lowering its zeta potential. This argument closely agree with the fact that the depressant effect of the water glass and its products on the mineral gangue is basically derived from the adsorption of the silicate containing hydrophilic colloids $(SiOH)_4$ on the surfaces of the gangue minerals and hence rendering them hydrophilic [52,53].

It could further be inferred that the depressing effect of SM on the surface of almandine was attributed to two main action mechanism: The first explanation could be due to formation of a stable hydrophilic complex of sodium metasilicate with metal ions from the surface of almandine such Fe^{3+}, Fe^{2+}, since, the active silicates ions in the depressant have a very good capacity of complexation with metal ions, such as iron ions, calcium ions, magnesium ions, and other active metal ions, which generate soluble complexes [23,54-56].

The specimens [SiO $(OH)_3^-$] and [SiO_2 $(OH)_2^{2-}$] present in metasilicate solution might have reacted with $Fe^{3+}$and Fe^{2+} ions to form the hydrophilic complexes $\equiv FeH_3SiO_4$ and $\equiv FeH_2SiO_4^-$, respectively on the almandine surface which further impaired the collector adsorption. Secondly, sodium metasilicate ions could also get adsorbed on the surface of almandine mineral, and thus changing the electrical properties of its surface. It may be assumed that $Fe^{2+,}$ which is the main active sites in almandine surface, may dissolve significantly in (Na_2SiO_3) solution. As the negative charges increases with the decrease in Fe^{2+} on the almandine surface, the electrical property of almandine will be totally altered altogether .The further assumption is that the complexes reactions will proceed as shown in the equations 3-6.

$$Fe-OH\ +Si(OH)_4 \leftrightarrow FeSiO\ (OH)_3\ +H_2O\ (l) \quad (3)$$

$$Fe-OH\ +SiO\ (OH)_4 \leftrightarrow FeSiO_2(OH)_2\ +H_2O\ (l) \quad (4)$$

To further explain the possible surface complexes which might have led to the depression of almandine floatability, see these ligand-exchange and complexes: ≡Fe-OSi $(OH)_2$OX or $(\equiv FeO)_2$-Si(OH)OX for the reactions between silicate monomers and almandine surface. The following ligand-exchange reactions may be proposed as well to expand on the knowledge of the reactions.

$$\equiv Fe-OX+H-OSi(\mathrm{OH})_2OX \Leftrightarrow \equiv Fe-OSi(\mathrm{OH})_2OX+HO-X \quad (5)$$

$$2(\equiv Fe-OX)+(H-O)_2Si(\mathrm{OH})OX \Leftrightarrow (\equiv Fe-O)_2-Si(\mathrm{OH})OX+2HO-X \quad (6)$$

XPS Analysis of Minerals Treated With and Without Sodium Metasilicate

To validate the adsorption mechanism of sodium metasilicate on minerals, the XPS analysis test was conducted. The XPS results of the almandine and rutile treated with and without sodium metasilicate are given in [Figure 9-12] as well as [Table 2,3] respectively. The survey spectrum in (Figure 9a,b) clearly revealed that the rutile structure is mainly composed of Ti and O. The C peak (284.60 eV) in the rutile could be due to the surface contaminants formed by exposure to air of the rutile sample and the hydrocarbons from the XPS instrument itself [57,58].

Table 2: XPS characterization of almandine before and after interacting with Na_2SiO_3.

Samples	Assignments	C1s	O1s	$Fe2p_{1/2}$	$Fe2p_{3/2}$	Si2p	Al2p
Almandine	Binding Energy/ eV	284.80	530.88 532.39	723.60 728.31	710.18 714.14	101.78 102.65	74.24
Almandine + SM	Binding Energy/ eV	284.80	530.32 532.80	722.70 728.00	709.95 713.95	101.89 102.98	74.25
Change	Binding Energy/ eV	-	+0.56 +1.59	-0.90 -0.31	+0.23 +0.19	+0.11 -0.33	0.01

Table 3: XPS characterization of rutile before and after interacting with Na_2SiO_3.

Samples	Assignments	C1s	O1s	Ti2p
Rutile	Binding Energy/eV	284.80	529.59 531.49 -	458.27 463.97 471.19
Rutile+ Na_2SiO_3	Binding Energy/eV	284.80	529. 65 531.32 -	458.38 464.09 471.42
Change	Binding Energy/eV	-	-0.06 -0.16	+0.11 +0.12 +0.23

The high-resolution XPS spectra of O, Ti, from (Figures 10a,b), are major part of the oxygen presented on the rutile and adsorbed water surface at all potentials included O^{2-}- and OH^- species. The XPS spectrum of Ti_2p peaks at potentials of 458.27 eV and 463.97 eV and 471.19 eV treated with SM while peaks 458.38 eV, 464.09 eV and 471.42 eV untreated with SM is shown in (Figure 10b). Characteristic of these peaks is obviously attributed to the XPS spectrum of Ti_2p in TiO_2 [59]. While the peak at 529.59 eV treated with SM and 529.65 eV untreated with the same SM, in (Figure 10a), is basically ascribed to the lattice oxygen in crystalline TiO_2 while the other peak at 531.49 eV treated with SM, and 531.32 eV treated with SM in the same (Figure 10a). Could be assigned to the surface hydroxyl groups, physically water and adsorbed oxygen species [60].

The binding energy peaks of iron (Fe), aluminium (Al), oxygen (O) could be detected on almandine surface respectively. Some of traces of O and C present in the almandine surface could be attributed to external pollution of instrument and atmosphere as well [58]. (Figure 11a,b), and c present the Fe_2p, Al_2p and O1s spectra of the almandine before and after treatment with SM respectively. Consequently, the Al(2p) spectrum is shown in

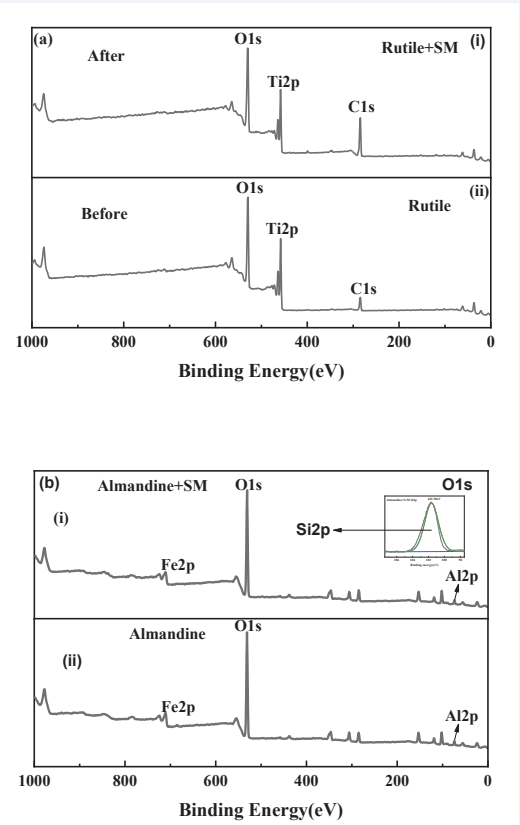

Figure 9 XPS survey spectra of (a) rutile and (b) almandine in the presence and absence of SM.

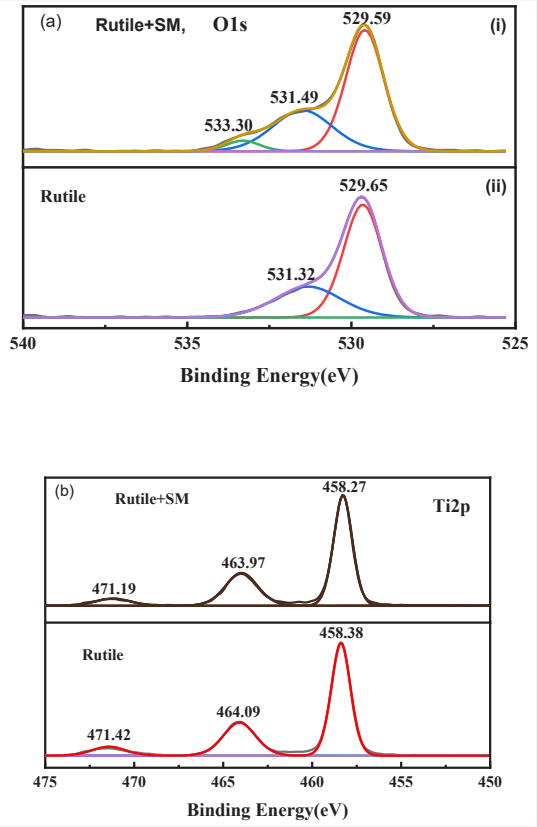

Figure 10 High resolutions spectra of (a) O1s and (b) Ti 2p on the rutile surface before and after SM treatment.

(Figure 11c (i)). Exhibits a peak at 74.20 eV when treated with reagent SM, which is basically ascribed to $Al_2p_{3/2}$ in Al-OH/O at the surface of almandine [61,62].

The binding energy before SM treatment was 74.19 eV in (Figure 11c (ii)), this reaffirms very negligible change of 0.01 eV clearly indicating that the element Al in the almandine surface does not react with any species of (Na_2SiO_3). In (Figure 11a), Fe_2p of untreated surface show peak of 710.18 eV which is assigned to $Fe_2p_{3/2}$ suggesting coexistence of Fe^{2+} and Fe^{3+} which are the active elements in almandine mineral [63,64]. In the same (Figure 11a), the peaks located at 710.18 eV and 723.60 eV corresponded to the binding energy of $Fe_2p_{3/2}$ and $Fe_2p_{1/2}$ [65, 66].

However, after being treated with the depressant at pH = 6, this broad band shifted to 709.95 eV binding energy, which may be assigned to elements, $Fe(OH)_3$, Fe_2O_3 or Fe_2O_4 and $FeOOH$ among others which are collectively referred to as iron 'ox hydroxide' [67,68]. These elements form the bulk of hydrophilic layers which are basically associated with the depression of almandine. Peak 713.95 eV may also be ascribed to $FeOOH$ [69], which may mean that after reaction sodium metasilicate, almandine formed a hydrophilic layer making it impossible for the adsorption of the collector. The other elements in the reaction with depressant are: 714.14 eV which is assigned to $Fe_2p_{3/2}$ as well. The change in the peaks exhibits a chemical change. The peaks which were observed at; 723.60 eV and 728.31 eV are basically attributed to $Fe_2p_{1/2}$. Based on the variation in the binding energy of peaks it can conclude that there was a chemical adsorption of depressant onto the surface of almandine. The changes are clearly depicted in (Table 3,4). The peak of O1s in (Figure 11b) without Na_2SiO_3 treatment was 530.88 eV which might be ascribed to iron ox hydroxide belonging to $Fe(OH)_3$ and $Fe_3Al_2(SiO_4)_3$ [70,71]. After deconvolution and the treatment with the depressor the

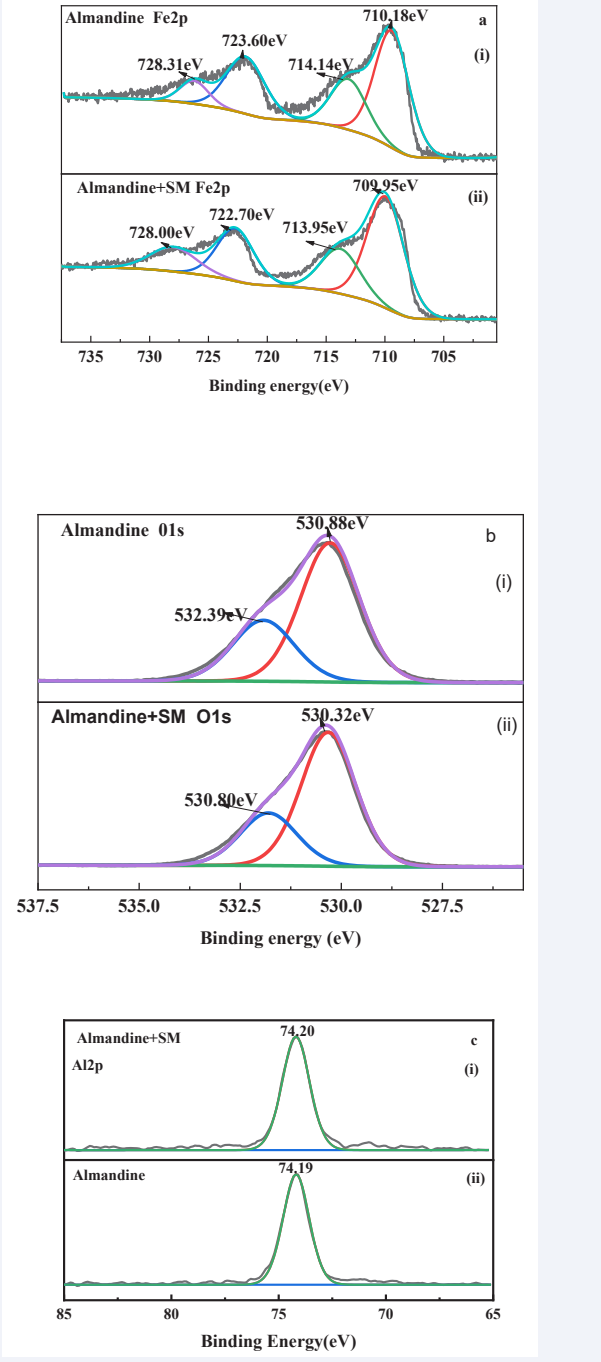

Figure 11 High-resolution XPS spectra of a. Fe 2p, b. O 1s and c. Al 2p on almandine surface before and after treatment with SM.

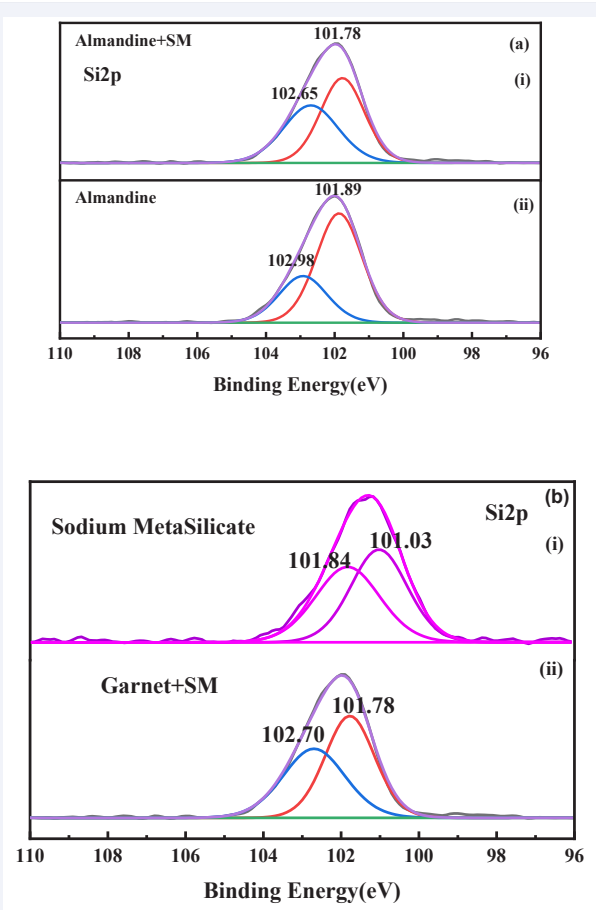

Figure 12 High-resolution XPS spectra of (a) Si2p, on (b) almandine surface before and after treatment with sodium metasilicate.

new peaks appeared at 530.32 eV, which is assigned to *FeOOH* [72,73]. The peak at 532.80 eV before treated with depressant changed to 530.39 eV after the treatment and this is basically ascribed to Fe_2SiO_4.

(Figure 12a,b) displays the Xps test for element Si_2p in the sodium silicate depressant and how it interacted with almandine mineral gangue. The binding energy of the Si_2p peaks before depressant interacted with almandine is located at 101.03 eV and 101.84 eV, after the interaction with sodium metasilicate the peaks shifts to 101.78 eV and 102.70 eV which indicated that there was the formation of pure iron silicates [40], which are hydrophilic in nature and produced the depression of almandine surface. It can be therefore inferred that a (Si_2p) element in SM, interacted with almandine surface through chemical bonding to cause depression of the almandine floatability.

CONCLUSION

The results of single micro flotation tests revealed that almandine and rutile had similar floatability characteristics when AC1815 was utilized as the collector that is, the floatabilities increased as the collector concentration was increased in both cases. Similarly, zeta potential results on the other hand, have demonstrated that adsorption of anions of either [$SiO(OH)_3^-$], [$SiO_2(OH)_2^{2-}$] and [$SiOH^-$] might have played a critical and key role in the depression of almandine under flotation pH range (pH = 4-8) through electrostatic force. Depressant-almandine complexes might have taken place in form of ligand-exchange: ≡Fe-O$Si(OH)_2$OX or ($\equiv FeO)_2$-Si(OH)OX which could have contributed further to depression of almandine floatability. Contact angle measurements demonstrated that the surface of almandine became more hydrophilic than that of rutile when both minerals were treated with sodium metasilicate.

A further observation from XPS analysis was that, a (Si_2p) element in sodium metasilicate interacted with almandine surface through chemical bonding to cause depression of the almandine floatability. Finally, the adsorption of sodium metasilicate in almandine surface through chemisorption might have caused the depression of its floatability by reducing the number of Fe active sites for collector attachment and adsorption.

ACKNOWLEDGEMENT

This work was funded by the Natural Science Foundation of China (projects Nos.51904208, 51974205) and The Open Foundation of State Key Laboratory of Mineral Processing (BGRIMM-KJSKL-2021-16). This research is also supported by International Science and Technology Cooperation Program of Hubei Province (project No.2022EHB016).

REFERENCES

1. Hosten C. Micro-floatability of rutile and zircon with soap and amine type collectors. Physicochem. Probl Miner Process. 2001; 35: 161-170.
2. Wang Y, Wen S, Zhang J, Wu D, Xian Y, Shen H. Flotation behaviour and surface characteristic of anosovite in a sodium oleate solution. Physicochem. Probl Miner Process. 2017; 53: 714-723.
3. Wei XIAO, Pan CAO, Qian-nan LIANG, Xiao-tao HUANG, Kai-yun LI, Yan-sheng ZHANG, et al. Adsorption behavior and mechanism of Bi (III) ions on rutile-water interface in the presence of nonyl hydroxamic acid. Trans. Nonferrous Met Soc. 2018: 28: 348-355.
4. WANG, J, Tao J, Lin Z, Xiang-long Z, Yan-bin T, Yong W, et al. Review on Mineral Processing Technology of Rutile in China. 2017; 3: 410083.
5. Hao Ding, Hai Lin, Yanxi Deng. Depressing effect of sodium hexametaphosphate on apatite in flotation of rutile. J Univ Sci Technol. 2007: 14: 200-203.
6. Xu B, Liu S, Hongqiang L, Zhao Y, Li H, Song S. A novel chemical scheme for flotation of rutile from eclogite tailing. Results in physics. 2017. 7: 2893-2897.
7. Jun W. Flotation behavior and mechanism of rutile in presence of sodium oleate. Transactions of Nonferrous Metals Society of China. 2014; 24: 820-825.
8. Cheng H, Liu C, Guo Z, Feng A, Wei M, Lv Z, et al. Electrokinetic and flotation behavior of rutile in the presence of lead ions and aluminium ions. Physicochemical Problems of Mineral Processing. 2019; 55: 458-466.
9. Walpole EA, Stewart R. Synthetic rutile production from Murray Basin ilmenite by the Austpac ERMS process. Murray Basin mineral sands, extended abstracts. Mildura: Australian Institute of Geoscientists. 1999; 164-168.
10. Gonçalves, CC, Braga PFA. Heavy mineral sands in Brazil: deposits, characteristics, and extraction potential of selected Areas. Minerals. 2019; 9: 176.
11. Kasomo RM, Li H, Zheng H, Chen Q, Weng X, Mwangi AD, et al. Selective flotation of rutile from almandine using sodium carboxymethyl cellulose (Na-CMC) as a depressant. Minerals Engineering. 2020; 157: 106544.
12. Li H, Mu S, Weng X, Zhao Y, Song S. Rutile flotation with Pb2+ ions as activator: Adsorption of Pb2+ at rutile/water interface. Colloids and Surfaces A: Physicochemical and Engineering Aspects. 2016; 506: 431-437.
13. Chen Q, Tian M, Zheng H, Luo H, Li H, Song S, et al. Flotation of rutile from almandine using sodium fluorosilicate as the depressant. Colloids and Surfaces A: Physicochemical and Engineering Aspects, 2020; 599: 124918.
14. Chen Q, Kasomo RM, Li H, Jiao X, Zheng H, Xiaoqing Weng, et al. Froth flotation of rutile–An overview. Minerals Engineering. 2021; 163: 106797.
15. Zhai J, Chen P, Sun W, Chen W, Wan S. A review of mineral processing of ilmenite by flotation. Minerals Engineering. 2020; 157: 106558.
16. Rejith RG, Sundararajan M. Combined magnetic, electrostatic, and gravity separation techniques for recovering strategic heavy minerals from beach sands. Marine Georesources & Geotechnology. 2018; 36: 959-965.
17. Farrokhpay S. The significance of froth stability in mineral flotation—A review. Adv colloid interface sci. 2011; 166: 1-7.
18. Lotter NO, Whiteman E, Bradshaw DJ. Modern practice of laboratory flotation testing for flowsheet development–A review. Minerals Engineering. 2014; 66: 2-12.
19. Pattanaik A, Venugopal R. Role of Surfactants in Mineral Processing: An Overview. Surfactants and Detergents. 2019.
20. Liu Q, Peng Y. The development of a composite collector for the flotation of rutile. Minerals Engineering, 1999; 12: 1419-1430.

21. Yang Y, Xu L, Liu Y, Han Y. Flotation separation of ilmenite from titanaugite using mixed collectors. Separation Science and Technology. 2016; 51: 1840-1846.

22. Chen Q, Tian M, Kasomo RM, Li H, Zheng H, Song S, et al. Depression effect of Al (III) and Fe (III) on rutile flotation using dodecylamine polyxyethylene ether as collector. Colloids and Surfaces A: Physicochemical and Engineering Aspects. 020; 603: 125269.

23. Richard M Kasomo, Hongqiang Li, Huifang Zheng, Qian Chen, Xiaoqing Weng, Akisa D Mwangi, et al. Depression of the selective separation of rutile from almandine by Sodium Hexametaphosphate. Colloids and Surfaces A: Physicochemical and Engineering Aspects. 2020; 593: 124631.

24. Pavez O, Peres AEC. Effect of sodium metasilicate and sodium sulphide on the floatability of monazite-zircon-rutile with oleate and hydroxamates. Minerals engineering. 1993; 6: 69-78.

25. Rao DS, Vijayakumar TV, Angadi S, Prabhakar S, Raju GB. Effects of modulus and dosage of sodium silicate on limestone flotation. 2010; 4: 397-404.

26. Tohry A, Dehghan R, Chelgani SC, Rosenkranz J, Rahmani OA. Selective separation of hematite by a synthesized depressant in various scales of anionic reverse flotation. Minerals. 2019; 9: 124.

27. Zhang G, Gao Y, Chen W, Liu D. The role of water glass in the flotation separation of fine fluorite from fine quartz. Minerals. 2017; 7: 157.

28. Qun W, Heiskanen K. Batch flotation tests by fatty acid on a phosphate-iron oxide-silicate regolith ore sample from Sokli, Finland. Minerals engineering. 1990; 3: 473-481.

29. Fuerstenau MC, Han KN. Reagents in Mineral Technology. 2018; 411-428.

30. Cebeci Y, Bayat O. Effect of flotation reagents on the wet grinding of celestite concantrate. Indian journal of chemical technology. 2004; 11: 382-387.

31. Andrade EM, Costa BLCM, Alcântara GAG, Lima RMF. Flotation of manganese minerals and quartz by sodium oleate and water glass. Latin American applied research. 2012; 42: 39-43.

32. Chen W, Chen F, Xianzhong Bu, Zhang G, Zhang C, Song Y. A significant improvement of fine scheelite flotation through rheological control of flotation pulp by using garnet. Minerals Engineering. 2019; 138: 257-266.

33. Molifie A. Investigating the use of sodium metasilicate to improve the flotation performance of altered PGE ores. 2021.

34. Alsafasfeh A, Alagha L. Recovery of Phosphate Minerals from Plant Tailings Using Direct Froth Flotation. Minerals. 2017; 7: 145.

35. Xiao W, Fang C, Wang J, Liang Q, Cao P, Wang X, et al. The role of EDTA on rutile flotation using Al 3+ ions as an activator. Rsc Advances. 2018; 8: 4872-4880.

36. Wills BA, Finch J. Wills' mineral processing technology. An introduction to the practical aspects of ore treatment and mineral recovery. Butterworth-Heinemann. 2015.

37. Gorain B, Franzidis J, Manlapig E. Flotation Cell Design: Application of Fundamental Principles. Julius Kruttschnitt Mineral Research Centre. Indooroopilly. Queensland. Australia. 2000.

38. Mahltig B. Smart hydrophobic and soil-repellent protective composite coatings for textiles and leather. Smart composite coatings and membranes. 2016; 261-292.

39. Chau T. A review of techniques for measurement of contact angles and their applicability on mineral surfaces. Minerals Engineering. 2009; 22: 213-219.

40. Guo P, Wang C. Good lithium storage performance of Fe_2SiO_4 as an anode material for secondary lithium ion batteries. RSC advances. 2017; 7: 4437-4443.

41. Bai S, Ding Z, Xianyu Fu, Chunlong Li, Chao Lv, Wen S. Investigations on soluble starch as the depressant of hematite during flotation separation of apatite. Physicochem Probl Miner Process. 2019; 55: 35-48.

42. Abaka-Wood GB, Addai-Mensah J, Skinner W. A study of selective flotation recovery of rare earth oxides from hematite and quartz using hydroxamic acid as a collector. Advanced Powder Technology. 2018; 29: 1886-1899.

43. Bulatovic SM. Handbook of flotation reagents: chemistry, theory and practice. Chemical engineering. 2007; 1.

44. Rao SR, Leja J. Surface chemistry of froth flotation. Reagents and mechanisms. 2004.

45. Wenbao Liu, Xiangyu Peng, Wengang Liu, Xinyang Wang, Qiang Zhao, Benying Wang. Effect mechanism of the iso-propanol substituent on amine collectors in the flotation of quartz and magnesite. Powder Technology. 2020; 360: 1117-1125.

46. Bin Yang, Wan-Zhong Yin, Jin Yao, Zhang-Lei Zhu, Hao-Ran Sun, Ke-Qiang Chen, et al. Differential adsorption of a high-performance collector at solid–liquid interface for the selective flotation of hematite from quartz. Journal of Molecular Liquids. 2021; 339: 116828.

47. Su T, Chen T, Zhang Y, Peiwei Hu. Selective Flocculation Enhanced Magnetic Separation of Ultrafine Disseminated Magnetite Ores. Minerals. 2016; 6: 86.

48. Li F, Zhong H, Wang S, Liu G. The activation mechanism of Cu (II) to ilmenite and subsequent flotation response to α-hydroxyoctyl phosphinic acid. Journal of Industrial and Engineering Chemistry. 2016; 37: 123-130.

49. Kasomo RM, Li H, Chen Q, Soraya DA, Leopold M, Weng X, et al. Behavior and mechanism of sodium sulfite depression of almandine from rutile in flotation system. Powder Technology. 2020; 374: 49-57.

50. Owens CL, Nash GR, Hadler K , Fitzpatrick RS, Anderson CG, Wall F. Zeta potentials of the rare earth element fluorcarbonate minerals focusing on bastnäsite and parisite. Adv Colloid Interface Sci. 2018; 256: 152-162.

51. Yang Y, Xu L, Tian J, Liu Y, Han Y. Selective flotation of ilmenite from olivine using the acidified water glass as depressant. International journal of mineral processing. 2016; 157: 73-79.

52. Bo F, Xianping L, Jinqing W, Pengcheng W. The flotation separation of scheelite from calcite using acidified sodium silicate as depressant. Minerals Engineering. 2015; 80: 45-49.

53. Yang X, Roonasi P, Holmgren A. A study of sodium silicate in aqueous solution and sorbed by synthetic magnetite using in situ ATR-FTIR spectroscopy. J Colloid Interface Sci. 2008; 328: 41-47.

54. Gao Y, Zhang G, Wang M, Liu D. The Critical Role of Pulp Density on Flotation Separation of Nickel Copper Sulfide from Fine Serpentine. Minerals. 2018; 8: 317.

55. Lu YP, Zhang MQ, Feng QM, Long T, Ou LM, Zhang GY. Effect of sodium hexametaphosphate on separation of serpentine from pyrite. Transactions of Nonferrous Metals Society of China. 2011; 21: 208-213.

56. Yang X. Interactions between iron oxides and silicates. 2008.

57. Wang X, Plackowski CA, Nguyen AV. X-ray photoelectron spectroscopic investigation into the surface effects of sulphuric acid treated natural zeolite. Powder technology. 2016; 295: 27-34.

58. Liu W, Wenbao L, Wang X, Wei D, Wang B. Utilization of novel surfactant N-dodecyl-isopropanolamine as collector for efficient separation of quartz from hematite. Separation and Purification Technology. 2016; 162: 188-194.

59. Chen P, Zhai J, Sun W, Hu Y, Yin Z. The activation mechanism of lead ions in the flotation of ilmenite using sodium oleate as a collector. Minerals Engineering. 2017; 111: 100-107.

60. Chaturvedi A, Joshi MP, Mondal P, Sinha AK, Srivastava AK. Growth of anatase and rutile phase TiO_2 nanoparticles using pulsed laser ablation in liquid: influence of surfactant addition and ablation time variation. Applied Surface Science. 2017; 396: 303-309.

61. He H, Alberti K, Barr TL, Klinowski J. ESCA studies of aluminophosphate molecular sieves. The Journal of Physical Chemistry. 1993; 97: 13703-13707.

62. Zhang N, Ejtemaei M, Nguyen AV, Zhou C. XPS analysis of the surface chemistry of sulfuric acid-treated kaolinite and diaspore minerals with flotation reagents. Minerals Engineering. 2019; 136: 1-7.

63. Song H, Li Y, Lou Z, Xiao M, Hu L, Ye Z, et al. Synthesis of Fe-doped WO3 nanostructures with high visible-light-driven photocatalytic activities. Applied Catalysis B: Environmental. 2015; 166: 112-120.

64. Yu J, Xiang Q, Zhou M. Preparation, characterization and visible-light-driven photocatalytic activity of Fe-doped titania nanorods and first-principles study for electronic structures. Applied Catalysis B: Environmental. 2009; 90: 595-602.

65. Yamashita T, Hayes P. Analysis of XPS spectra of Fe^{2+} and Fe^{3+} ions in oxide materials. Applied surface science. 2008; 254: 2441-2449.

66. Seyama H, Soma M. Fe 2p spectra of silicate minerals. Journal of electron spectroscopy and related phenomena. 1987; 42: 97-101.

67. Pratt AR, Nesbitt HW, Muir IJ. Generation of acids from mine waste: Oxidative leaching of pyrrhotite in dilute H2SO4 solutions at pH 3.0. Geochimica et Cosmochimica Acta. 1994; 58: 5147-5159.

68. Miki H, Hirajima T, Muta Y, Suyantara GPW, Sasaki K. Effect of sodium sulfite on floatability of chalcopyrite and molybdenite. Minerals. 2018; 8: 172.

1. 2. Buckley AN, Woods R. An X-ray photoelectron spectroscopic study of the oxidation of chalcopyrite. Australian Journal of Chemistry. 1984; 37: 2403-2413.

69. Seyama H, Soma M. Bonding-State Characterization of the Constituent Elements of Silicate Minerals by X-Ray Photoelectron Spectroscopy. J Chem Soc. 1985; 81: 485-495.

70. Grano SR, Sollaart M, Skinner W, Prestidge CA, Ralston J. Surface modifications in the chalcopyrite-sulphite ion system. I. collectorless flotation, XPS and dissolution study. International journal of mineral processing. 1997; 50: 1-26.

71. Siriwardane RV, Cook JM. Interactions of SO2 with sodium deposited on CaO. Journal of colloid and interface science. 1986; 114: 525-535.

72. Lin S, Liu R, Bu Y, Wang C , Wang L , Sun W, et al. Oxidative Depression of Arsenopyrite by Using Calcium Hypochlorite and Sodium Humate. Minerals. 2018; 8: 463.